ELSEVIER

Chemical Engineering Journal 76 (2000) 77–86

Chemical Engineering Journal

www.elsevier.com/locate/cej

A novel interconnected fluidised bed for the combined flash pyrolysis of biomass and combustion of char ☆

Arthur M.C. Janse *, P. Maarten Biesheuvel, Wolter Prins, Wim P.M. van Swaaij

Department of Chemical Technology, University of Twente, P.O. Box 217, 7500 AE Enschede, The Netherlands

Received 7 March 1999; received in revised form 27 April 1999; accepted 25 May 1999

Abstract

A novel system of two adjacent fluidised beds operating in different gas atmospheres and exchanging solids was developed for the combined flash pyrolysis of biomass and combustion of the produced char. Fluidised sand particles (200 μm < d_p < 400 μm) are transported from the pyrolysis reactor to the combustor through an orifice and recycled by a standpipe, riser and cyclone. Advantages of the new design are its compactness and the high level of heat integration. The solids circulation rate and holdup distribution between the two compartments could be controlled adequately in experiments at room temperature and atmospheric pressure. A model, developed to predict the solids and gas exchange between the two reactor compartments, was validated with experiments in which the three relevant gas flows, the orifice diameter and the particle diameter were varied.

Keywords: Interconnected fluidised bed; Rotating cone reactor; Orifice; Standpipe; Biomass; Pyrolysis

1. Introduction

The flash pyrolysis of biomass to produce bio-oil is often performed in a bubbling fluidised bed [1,2] or a circulating fluidised bed [1,3,4]. In such reactors the biomass particles are heated rapidly and they have the advantage of a simple construction. A disadvantage is the large carrier gas stream which necessitates extra heating and large downstream equipment. To obviate these disadvantages, a novel reactor type was developed by Wagenaar et al. [5] which enables a high solids throughput without requiring any transport gas. The heart of this ‘rotating cone reactor’ consists of a rotating cone, in which biomass particles are mixed intensively with an excess of hot sand particles. The circulating hot sand provides the heat for the pyrolysis process and prevents fouling of the cone wall.

More recently, an advanced version of the rotating cone reactor was developed including an internal circulation of particles within the pyrolysis section [6–9] and an external circulation for char combustion [6,7,9] (see Fig. 1). In this concept, the rotating cone is partly submerged in a fluidised bed and sand flows through supply openings near the bottom of this cone. Due to centrifugal forces, sand particles flow along the cone wall in upward direction, pass the upper edge and fall back into the fluidised bed (the internal circulation loop).

Char that is produced during flash pyrolysis is normally blown out of the reactor and separated from the pyrolysis vapours by means of a cyclone or a hot gas filter [10]. However, the combustion of char may provide the energy necessary for the endothermic pyrolysis process which would enable an overall autothermal operation. To that end, an external circulation loop was introduced in the rotating cone reactor, combining the pyrolysis reactor with a section for char combustion. Char and sand are now transported through an orifice to the combustor where the sand is reheated before being recycled to the pyrolysis reactor by means of a standpipe, riser and cyclone.

This new concept is based on a development started by Kuramoto et al. [11,12] and Masson [13] who connected two fluidised bed reactors with different gas atmospheres by orifices and overflow baffles. Such a system is called an interconnected fluidised bed (*IFB*) and offers the advantage of compactness and a good integration of heat [14,15].

As the overflow baffles in an *IFB* fix the heights of the dense and adjacent lean beds, the pressure drop over orifices in the system can only be influenced by changes in bed porosity, thereby limiting the size of the ‘operating window’ for solids flow. Furthermore, the gas flow of so-called

☆ PII of original article S1385-8947(99)00095-9

* Corresponding author. Present address: DSM Food Specialties, P.O. Box 1, 2600 MA Delft, The Netherlands. Tel.: +31-15-279-3845; fax: +31-15-279-2219

E-mail address: arthur.janse@gist-brocades.infonet.com (A.M.C. Janse)

1385-8947/00/$ – see front matter
PII: S1385-8947(99)00128-X

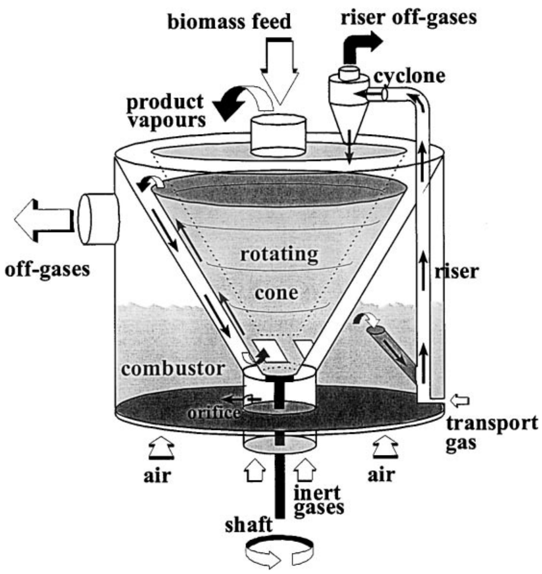

Fig. 1. Novel Rotating Cone Reactor. The pyrolysis reactor, containing the rotating cone, is surrounded by the combustor. Two sand circulations are maintained: the first one is located within the pyrolysis reactor, while the second circulation loop (the *IFB*-system) extents over both reactor compartments, the standpipe, riser and cyclone.

flushing and reactor beds are necessarily mixed in the joint freeboard, resulting in dilution of the produced vapours and larger downstream equipment for product collection. Nevertheless, for specific applications, the *IFB* is an attractive option.

In the rotating cone reactor set-up [6,7,9] an adjustment is made to the above design by replacing the overflow baffles by a small riser. From experiments it became clear that the solids circulation rate and holdup distribution could be controlled adequately and dilution of the product gas minimised.

It is the objective of this paper to investigate the transport characteristics of this new *IFB*-design. The exchange of solids and gas between the two interconnected fluidised beds is studied as well as the resulting solids holdup distribution. Gas flow through the orifice between the pyrolysis reactor (reductive atmosphere) and the combustor (oxidative atmosphere) is studied because this gas flow must be minimised to avoid the formation of explosive gas mixtures or a significant loss of the bio-oil vapours. Special attention is paid to the immersed small riser as this a non-standard piece of equipment. A small pilot plant was built in which the transfer of sand and gas could be measured at room temperature and atmospheric pressure. Transport models for standpipe flow and orifice flow are combined for a theoretical description of the transport behavior.

This paper focuses on the application of the novel *IFB*-design to the decomposition of biomass. However, applications in other fields (e.g., regenerative desulphurisation of power plant off-gases [14,15] or pyrolysis of mixed plastic waste [16,17]) are conceivable as well.

Table 1
Characteristic dimensions of the *IFB*-system, see also Fig. 3

Diameter rotating cone reactor	0.39 m
Height rotating cone reactor	0.40 m
Half cone top angle θ	30°
Diameter annular space in pyrolysis reactor $D_{outside}$	0.16 m
Diameter of shaft in pyrolysis reactor	0.09 m
Height annular space around shaft h_s	0.11 m
Inner diameter riser	0.02 m

2. Experimental

2.1. IFB-system

The characteristic dimensions of the *IFB*-system are listed in Table 1. Both beds were fluidised using compressed air. Orifices of different dimensions were used (1–4 cm ID). The pressure in the two compartments was measured at various heights with pressure taps and water manometers with an accuracy of $\sim$10 Pa. In the combustor 10 pressure taps were distributed over the height with a spacing of 1.5 cm, while the pyrolysis reactor had nine pressure taps. The pressure at the bottom and top of the riser were measured as well. Because the driving shaft of the rotating cone is submersed in a fluidised bed, a so-called labyrinth sealing was applied to prevent possible damage of the shaft construction. Such a sealing consists of an intricate connection between rotating cone and shaft in which gas flows outward through the sealing to prevent the movement of particles from the fluidised bed into the sealing. In our experiments always 50% of the gas flow to the pyrolysis reactor was directed through the labyrinth. In the experiments discussed in this work, the rotating cone only rotated at a very low velocity without transporting solids (the internal circulation, see above) but sufficient to equalise the bed level in the pyrolysis reactor. As a result, *IFB*-measurements could be interpreted more clearly and the complexity of the model confined.

2.2. Properties of sand

The physical properties of the sand particles are presented in Table 2. The sphericity factor ψ was derived by applying the Blake–Kozeny equation for the pressure gradient in a packed bed:

Table 2
Physical properties of sand particles

Particle diameter	220 μm	390 μm
Angle of repose α_r	31.6°	31.0°
Minimal fluidisation velocity U_{mf}	0.04 m/s	0.08 m/s
Density ρ_s	2490 kg/m^3	2605 kg/m^3
Packed bed porosity ε_0	0.40	0.40
Sphericity factor ψ	0.947	0.733

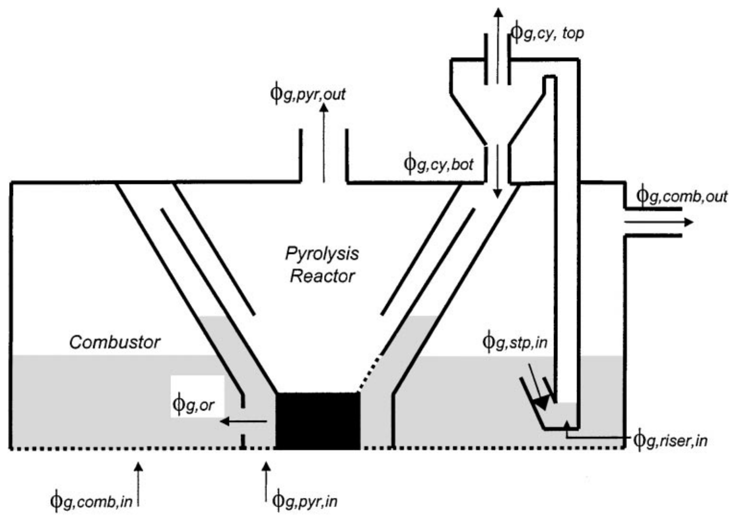

Fig. 2. Schematic representation of the rotating cone reactor showing the relevant gas flows.

$$\frac{\mathrm{d}P}{\mathrm{d}h} = 150\frac{(1-\varepsilon_0)^2}{\varepsilon_0^3}\frac{\eta}{(\psi d_\mathrm{p})^2}U \qquad (1)$$

and a momentum balance over a fluidised bed:

$$\frac{\mathrm{d}P}{\mathrm{d}h} = \rho_s(1-\varepsilon)g \qquad (2)$$

Here, P represents the pressure, h the vertical height, ε_0 the packed bed porosity, η the gas viscosity, d_p the particle diameter, U the superficial gas velocity, ρ_s the sand density, ε the fluidised bed porosity and g the gravity acceleration. The Blake–Kozeny equation was used because of the laminar character of the gas flow ($Re_\mathrm{p} < 10$). In both equations, friction of gas and solids with the wall is neglected. At minimum fluidisation ($U = U_\mathrm{mf}$), the pressure gradients dP/dh as given by Eq. (1) and (2) are equal and the porosity ε equals the packed bed porosity ε_0, giving the possibility to calculate ψ.

2.3. Measurement methods

The most important operating characteristics of the *IFB*-system at stationary conditions are the holdup distribution between the two compartments, the gas flow through the orifice and the solids circulation rate. The measurement of these parameters is now discussed.

Though the inner wall of the combustor has an inclination from 11 cm above the gas distributor (see Figs. 1 and 2), the combustor can be considered a vessel with straight vertical walls because the fluidised bed in this vessel was never much higher than 11 cm. With this information, the holdup in the combustor M_comb can be calculated from the bed height h_comb and the cross-sectional area A_comb by $M_\mathrm{comb} = h_\mathrm{comb}A_\mathrm{comb}\rho_\mathrm{s}(1-\varepsilon)$. The bed height follows from integration of either Eq. (1) or Eq. (2). The pyrolysis reactor has sloped walls and its holdup M_pyr can only be calculated indirectly. When the holdup in the riser and on the rotating cone wall is neglected, M_pyr equals the difference between the total holdup of the system M_sys and M_comb: $M_\mathrm{pyr} = M_\mathrm{sys} - M_\mathrm{comb}$.

In principle, the gas flow through the orifice, $\phi_\mathrm{g,or}$, can be determined from a volume balance over either the pyrolysis reactor or the combustor (see Fig. 2):

$$\phi_\mathrm{g,or} = \phi_\mathrm{g,pyr,in} - \phi_\mathrm{g,pyr,out} + \phi_\mathrm{g,cy,bot} \qquad (3)$$

$$\phi_\mathrm{g,or} = \phi_\mathrm{g,comb,out} - \phi_\mathrm{g,comb,in} + \phi_\mathrm{g,stp,in}$$

Unfortunately, these balances could not be used for the following reasons: 1. The balance over the pyrolysis reactor failed because the gas flow from the bottom side of the cyclone could neither be measured nor neglected, and 2. The combustor balance failed because the orifice flow is much too small in comparison with the combustor flow resulting in an unacceptable large measurement error. As a final solution, CO_2 was injected continuously as a tracer in the gas flow to the pyrolysis reactor $\phi_\mathrm{g,pyr,in}$ and a CO_2-balance was set up for the combustor:

$$(\phi_\mathrm{g}C)_\mathrm{or} + (\phi_\mathrm{g}C)_\mathrm{comb,in} = (\phi_\mathrm{g}C)_\mathrm{comb,out} + (\phi_g C)_\mathrm{stp,in} \qquad (4)$$

If it is assumed that:

1. The tracer concentration in the pyrolysis reactor $C_\mathrm{pyr,in}$ equals the concentration of the gas flow through the orifice C_or,
2. The tracer concentration in the gas flow to the combustor $C_\mathrm{comb,in}$ equals the concentration in air C_air,
3. The gas flows to and from the combustor are nearly equal: $\phi_\mathrm{g,comb,in} = \phi_\mathrm{g,comb,out}$,
4. The gas flow through the standpipe is very small with respect to the gas flow through the combustor: $\phi_\mathrm{g,stp} \ll \phi_\mathrm{g,comb}$,

then Eq. (4) can be simplified to:

$$\phi_\mathrm{g,or} = \frac{\phi_\mathrm{g,comb,out}(C_\mathrm{comb,out} - C_\mathrm{air})}{C_\mathrm{pyr,in}} \qquad (5)$$

Table 3
Base case for experimental work and simulations

Total sand holdup M_{sys}	25 kg
Pyrolysis reactor gas velocity	1.37 U_{mf}
Combustor gas velocity	1.78 U_{mf}
Riser gas velocity	4.1 m/s
Particle diameter	390 μm
Orifice diameter	2 cm

All parameters on the RHS were measured simultaneously to determine the orifice gas flow. It should be emphasised that a reverse gas flow, from the combustor to the pyrolysis reactor, cannot be detected by this experimental procedure.

The solids circulation rate was measured by putting a basket underneath the cyclone and measuring the collected amount of sand in a specified time interval. The only restriction for this method is that enough sand is collected for an accurate measurement, during a time period for which the system parameters remain essentially unchanged. This can be accomplished by collecting about 1% of the system holdup (see Table 3).

3. Theoretical background

In this section, equations are developed to describe the transport phenomena of the basic elements in the *IFB*-system (i.e., the orifice and the sandpipe) and validated with experiments. First, pressure profiles in the combustor and in the pyrolysis reactor are discussed.

3.1. Pressure profile in the combustor

The pressure profiles in the pyrolysis reactor and the combustor should be described accurately, because the flow of solids through the orifice is determined by the pressure difference over the orifice, while this pressure difference is small compared to the absolute pressures in both compartments. To describe the pressure profiles, first the influence of gas velocity on the bed porosity ε must be determined. The porosity was measured for each sand particle type from the height of a fluidised bed of known mass M, using the equations in Sections 2.2 and 2.3, which results in the following correlations:

$$\varepsilon=\varepsilon_0 \quad \text{for} \quad U<U_{\mathrm{mf}}, \quad \varepsilon=a+b\frac{U}{U_{\mathrm{mf}}} \quad \text{for} \quad U>U_{\mathrm{mf}}, \quad \varepsilon_0=0.40;\ a=0.361;\ b=0.038 \tag{6}$$

For the combustor, having straight walls, bed pressure profiles are now accurately described by Eq. (1) and (2).

3.2. Pressure profile in the pyrolysis reactor

Due to the conical shape of the upper part of the pyrolysis reactor, pressure profiles are somewhat harder to calculate.

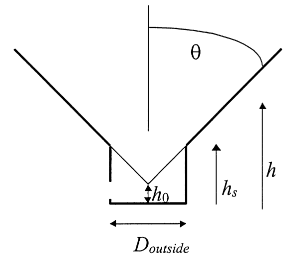

Fig. 3. Schematic representation of pyrolysis reactor. Symbols are described in Section 3.2 and Table 1. In this picture the outside measures of the reactor are given (i.e., the wall separating both compartments) without showing the rotating cone and the labyrinth sealing.

The procedure starts with the determination of the total bed height in the pyrolysis reactor h_{pyr}, and the determination of the height h_1 at which the gas velocity U becomes equal to U_{mf}, see Fig. 3.

The height h_{pyr} is calculated from the bed volume in the pyrolysis reactor V_{pyr}:

$$h_{\mathrm{pyr}}=h_0+\left(\frac{V_{\mathrm{pyr}}-A_{\mathrm{bot}}h_{\mathrm{s}}}{(\pi/3)\tan^2\theta}+(h_{\mathrm{s}}-h_0)^3\right)^{1/3} \tag{7}$$

Here, θ stands for the half top angle of the reactor, A_{bot} for the surface area at the bottom of the bed, h_0 for the virtual tip of the cone (i.e. $h_0=h_{\mathrm{s}}-(1/2)D_{\mathrm{outside}}/\tan\theta$), h_{s} for the height at the transition point conical part – cylindrical part and D_{outside} for the outside diameter of the annular space. In the conical part, the gas velocity $U(h)$ is a function of the gas flow ϕ and the available surface area $A(h)$: $U(h)=\phi/A(h)$. Here, $A(h)$ is $A(h)=\pi\tan^2\theta\ (h-h_0)^2$. Height h_1 now follows from setting U equal to U_{mf}:

$$h_1=h_0+\sqrt{\frac{\phi}{U_{\mathrm{mf}}\pi\tan^2\theta}} \tag{8}$$

The description of the inner bed pressure profile is divided into three parts, corresponding to different sections of the bed:

1. The lowest bed section consists of the small annular space surrounding the labyrinth with a height h_{s} and surface area A_{bot}. The pressure drop over this part is given by integration of either Eq. (1) or Eq. (2), depending on the applied gas velocity.
2. In case the gas velocity in the bottom section exceeds U_{mf}, a middle section is defined where the gas velocity exceeds the minimum fluidisation velocity ($U>U_{\mathrm{mf}}$ from h_{s} to h_1). The pressure difference over this section can be calculated from Eq. (2) and (6):

$$\Delta P=\rho_{\mathrm{s}}g(1-a)(h_1-h_{\mathrm{s}})+\frac{\rho_{\mathrm{s}}gb\phi}{U_{\mathrm{mf}}\pi\tan^2\theta}\left(\frac{1}{h_{\mathrm{s}}-h_0}-\frac{1}{h_1-h_0}\right) \tag{9}$$

3. The gas velocity is below the minimum fluidisation velocity ($U<U_{\mathrm{mf}}$) in the top section (from h_1 to h_{pyr}).

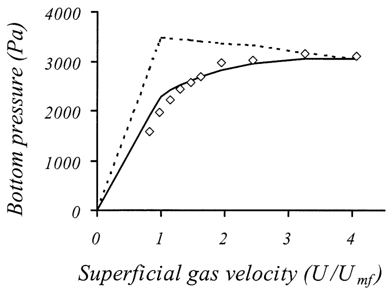

Fig. 4. Calculated (lines) and measured (symbols) values of the bottom pressure in the pyrolysis reactor. The holdup M_{pyr} is 10 kg and the gas velocity is based on the cross-sectional area of the annular bed surrounding the shaft A_{bot}. The dashed line is derived for a vessel with vertical walls, while the continuous line is based on a bed with partly sloped walls (Eqs. (7)–(10)).

The pressure drop over this section follows from integration of Eq. (1):

$$\Delta P = 150\frac{(1-\varepsilon_0)^2}{\varepsilon_0^3}\frac{\eta}{(\psi d_p)^2}\frac{\phi}{\pi\tan^2\theta} \times \left(\frac{1}{h_1-h_0}-\frac{1}{h_{pyr}-h_0}\right) \qquad (10)$$

In Fig. 4, measured bottom pressures in the pyrolysis reactor are compared with Eqs. (1) and (2) on the one hand, and Eqs. (9) and (10) on the other. It is clear that the latter equations describe the pressure profile better.

3.3. Solids flow through an orifice

The description of flow of solids and gas from a fluidised bed through an orifice to the atmosphere is based on a mechanical energy balance and leads to [4,14,18,19]:

$$\phi_s = C_d A_o \sqrt{2\rho_s(1-\varepsilon)\Delta P_o} \qquad (11)$$

Here, ϕ_s represents the solids flow, A_o the orifice surface area and ΔP_o the pressure difference over the orifice. The discharge coefficient C_d accounts for wall friction and flow contraction [20] and depends on the particle size and type, orifice diameter and the shape of the orifice. C_d-values are typically in between 0.4 and 0.7. Granular flow through an orifice between two adjacent fluidised beds can also be described by Eq. (11) [5,10,12,21–25].

In this paper the model developed by Korbee et al. [4,14] is used for orifice flow from either a fluidised or a packed bed to another fluidised bed. The model is not derived again for reasons of conciseness. However, two adjustments are made to the Korbee-model which we will now discuss. First, Korbee et al. incorporated the solids pressure, σ_x, originating from the weight of solids above the orifice, in Eq. (11):

$$\phi_s = C_d A_o \sqrt{2\rho_s\,(1-\varepsilon)\,(\sigma_x+\Delta P_o)} \qquad (12)$$

We argue that a solids phase pressure should not be implemented in Eq. (11) for the following reasons:

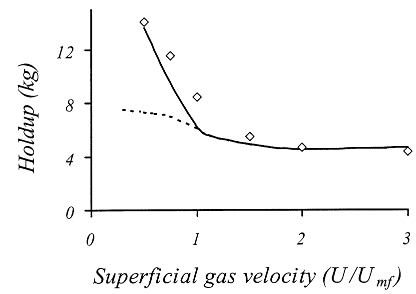

Fig. 5. Holdup in the pyrolysis reactor M_{pyr} as a function of the gas velocity. Comparison of model calculations with (- - -) and without (—) a solids phase pressure, to the results of direct measurements. Operating conditions are listed in Table 3.

- Several authors have measured solids flow through an orifice from non-aerated beds [12,23,26,27] and were able to describe the experiments adequately with Eq. (11).
- The Korbee-model [4] was re-evaluated by us and it was shown that the solid phase pressure had practically no influence on the outcome, because the value of the (static) friction factor used in the study by Korbee was very high (f = 2.4). Using the set-up described by Korbee (p. 5830) to measure f, we found f = 0.17 for ballotini glass as well as for sand particles (200–400 μm).
- For this work, a complete *IFB*-model (see Section 3.5) was made with a submodel for the gas and solids transport through the orifice as a critical part. Two variants were tested for the description of flow through the orifice model, one with and one without the solids phase pressure. Fig. 5 shows the measured holdup of the pyrolysis reactor as a function of the gas velocity for the base case (Table 3) and the predictions for the two variants of the orifice-model. The variant without a solids phase pressure describes measurements much better, which indicates that the solids pressure must be omitted from a description of the orifice flow.
- The fact that a solids pressure, though obviously present in a partly fluidised bed ($U < U_{mf}$), does not act as a driving force for flow in horizontal direction, can be understood from the non-elasticity of the rigid solid particles. Particles, near the orifice, which are accelerated due to the pressure of gas (and solids) through the orifice, will loose contact. This notion is visualised very schematically in Fig. 6. Consequently, the solids pressure cannot exert work and should be omitted from the mechanical energy balance.

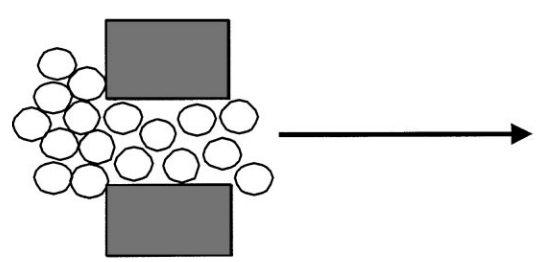

Fig. 6. Particle concentration variation near the orifice.

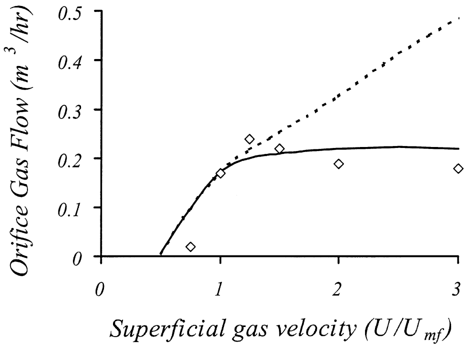

Fig. 7. Gas flow rates through the orifice as a function of the gas velocity in the pyrolysis reactor. Comparison of model calculations with the dense bed porosity ε (- - -) and the packed bed porosity ε_0 (—) with experimental data.

- This above observation is confirmed by research of Kuvshinov [28] who studied the free flow of granular material through an orifice. He observed that the solids flow does not depend on the nature of the particle motion in front of the orifice but is determined by the emergence of particles from the dense bed into the free space. Only drag of percolating gas was a driving force. Also, Molodtstof et al. [29] studied the vertical flow of solids through orifices from hoppers and came to the conclusion that the normal component of intergranular stress is zero in the direction of particle flow.

Based on the above references, our own measurements and the evaluation of Korbee's model, we left out the solids phase pressure as a driving force for orifice flow.

The second (minor) adjustment to the Korbee-model made in this work, concerns the porosity of the orifice flow. Korbee used the porosity of the dense bed $\varepsilon(\varepsilon \geq \varepsilon_0)$ for the description of the porosity of orifice flow. Instead, our experiments were better described if the packed bed porosity ε_0 was used. This can be concluded from Fig. 7, which shows the gas flow through the orifice as a function of the gas velocity through the pyrolysis reactor as predicted by the *IFB*-model (see Section 3.5). It seems as if particle flow is densified toward the orifice, up to the packed bed density, before particles accelerate in the orifice and loose contact. Densification of granular flow was also observed by Martin and Davidson [30] who investigated the flow of solids through orifices from a fluidised bed to the atmosphere. Using several types of nozzles, they sometimes noticed a decrease of the voidage to below the minimum fluidisation voidage. Burkett et al. [31] also observed a porosity decrease toward the orifice.

3.4. Solids flow through a standpipe

The standpipe geometry can be seen in Figs. 1 and 2. This very short inclined standpipe is submerged in the fluidised combustor, feeding a riser without any control valve or restriction. Important entrance and exit effects can be expected and no literature correlations are available for this specific case, except perhaps from Sarkar et al. [32–34] who measured solids flow from a silo to the atmosphere through an inclined standpipe. In fact, our short standpipe forms an obstacle for gas flow from the combustor to the riser while, by the presence of a dense bed inside it, it may also provide for the driving force for solids flow from the combustor to the riser.

To analyze the situation, we will start with a macroscopic mechanical energy balance for the solid phase:

$$\Delta\left(\tfrac{1}{2}\rho v^2\right) + \Delta P_{\mathrm{stp}} + \Delta\sigma_{\mathrm{s}} + \Delta(\rho g h) = -E_{\mathrm{f}} \qquad (13)$$

Here ΔP_{stp} represents the difference between the fluidised bed pressure at the top of the standpipe $P_{\mathrm{stp,comb}}$ and the pressure at the bottom of the riser $P_{\mathrm{bot,riser}}$: $\Delta P_{\mathrm{stp}} = P_{\mathrm{stp,comb}} - P_{\mathrm{bot,\ riser}}$while $\Delta\sigma_{\mathrm{s}}$ stands for the solids phase pressure, h the vertical height of the standpipe and E_{f} for the sum of all frictional losses. When the solids are considered to flow as a moving packed bed, not supported by the gas phase or walls, the weight of the solids is counterbalanced by the solids pressure σ_{s} on the bottom of the standpipe/riser: $\sigma_{\mathrm{s,bot,riser}} = -\Delta(\rho g h)$. If all friction and in/outlet effects (thus E_{f}) are taken into account by means of a discharge coefficient, then the following equation for the flux of solids can be derived from Eq. (13):

$$\Phi'' = C_{\mathrm{d}}\sqrt{2\rho_{\mathrm{s}}(1-\varepsilon_0)\Delta P_{\mathrm{stp}}} \qquad (14)$$

Eq. (14) was tested against experimental data before being introduced into the *IFB*-model. Measurements were performed with varying riser gas velocity (up to 12 m/s) and varying bed heights above the standpipe entrance (up to 10 cm). Fig. 8 shows that sand flow rates through the standpipe, riser and cyclone, plotted versus the corresponding pressure difference over the standpipe, deviate considerably from the values obtained while using Eq. (14) with $C_{\mathrm{d}} = 0.15$. Solids flow even occurred at negative pressure drops over the standpipe, especially at high riser gas velocities (>7 m/s). At such conditions, gas bubbles could be seen to escape from the standpipe to the fluidised bed. Obviously, a part of the riser gas flow slipped through the standpipe. In general, this phenomenon occurred when the pressure drop over the

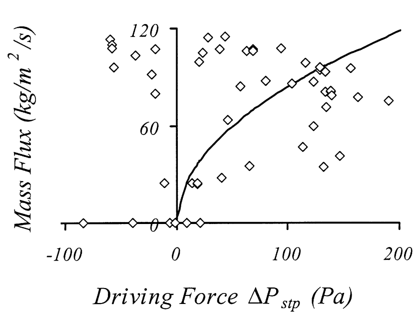

Fig. 8. Transport of sand ($d_{\mathrm{p}} = 390$ μm) through the standpipe as a function of the driving force. For all experiments this driving force is given by ΔP_{stp}, according to Eq. (14).

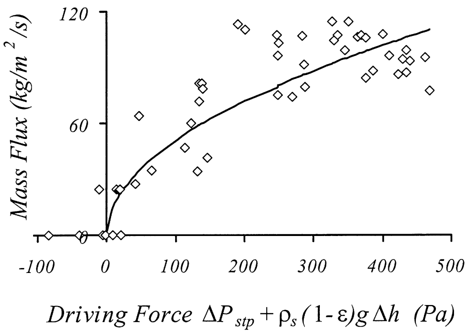

Fig. 9. Transport of sand (d_p = 390 μm) through the standpipe as a function of the driving force. For experiments in which bubbles emerged from the standpipe, the driving force as given by Eq. (15) is used.

riser was high in comparison with the pressure drop over the standpipe. Presumably, in this case, a partly fluidised bed moves through the standpipe, instead of a packed bed. As a consequence, the solids pressure will be absent and does not compensate the weight of solids in the standpipe. Eq. (14) is then no longer valid and an additional term should be included in the expression for the solids flow through the orifice to take the gravity force into account:

$$\Phi'' = C_d\sqrt{2\rho_s(1-\varepsilon)(\Delta P_{stp} + \rho_s(1-\varepsilon)g\Delta h)} \qquad (15)$$

Fig. 9 is similar to Fig. 8, but is now based on Eq. (15) for all measurements in which gas bubbles were seen to emerge from the standpipe. Here, Δh stands for the vertical height difference between entrance and exit of the standpipe. The values of C_d, ε and Δh used, are 0.12, 0.40 and 2 cm, respectively. A comparison between Figs. 8 and 9 reveals the improvement of Eq. (15) with respect to Eq. (14). Although data are scattered and the model can only be looked upon as a first approximation, the result is satisfying considering the large in- and outflow effects. It must be realised that the standpipe has a length of only 5 cm.

3.5. *IFB-model*

To describe sand transfer between the two compartments, a model is devised that combines two submodels, one for the orifice flow and one for the standpipe flow. Both submodels and the overall model are iterative by nature. For a certain starting value of the holdup distribution, mass flows through orifice and standpipe are calculated. Based on the outcome, a new holdup distribution is calculated until a stationary situation is reached. An input in the standpipe sub-model is the pressure difference over riser and cyclone as a function of the solids mass flow and riser gas velocity. This could not be modelled separately; thus separate flow experiments were done with the standpipe/riser/cyclone-system with the standpipe submersed in a fluidised bed (see Appendix A).

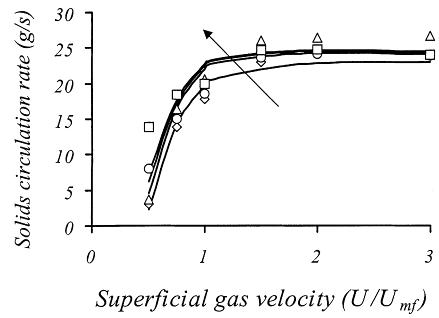

Fig. 10. Influence of the pyrolysis reactor gas velocity on the solids circulation rate in the *IFB*-system for various orifice diameters. The following symbols are used in Figs. 10–13: (◇) 1 cm, (△) 2 cm, (○) 3 cm, (□) 4 cm. Lines refer to model calculations and the arrow indicates an increasing orifice diameter. The operating conditions from Table 3 are valid for Figs. 10–15.

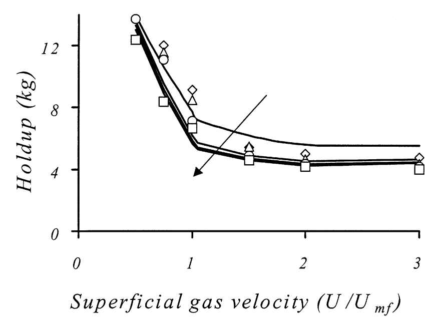

Fig. 11. Influence of the pyrolysis reactor gas velocity on the holdup in the pyrolysis reactor for various orifice diameters. See Fig. 10 for explanation of symbols.

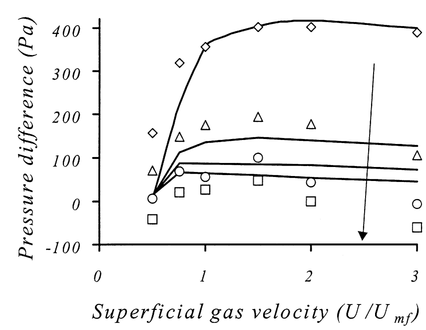

Fig. 12. Orifice pressure difference as a function of the pyrolysis reactor gas velocity for various orifice diameters. See Fig. 10 for explanation of symbols.

4. Results

In the experimental program, the gas flow rates to the pyrolysis reactor, combustor and riser, the orifice diameter and the sand particle size were varied starting from the base case of Table 3. In this work only the influence of orifice size, pyrolysis reactor gas velocity and particle size will be discussed. Figs. 10–13 show measurements and model calculations on the influence of the gas velocity in the pyrol-

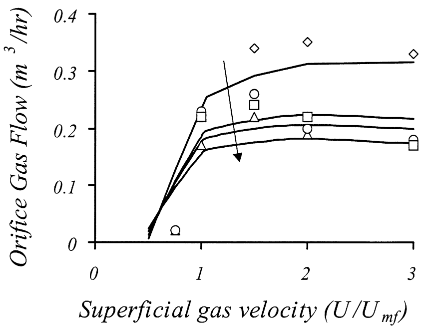

Fig. 13. Orifice gas flow as a function of the pyrolysis reactor gas velocity for various orifice diameters. See Fig. 10 for explanation of symbols.

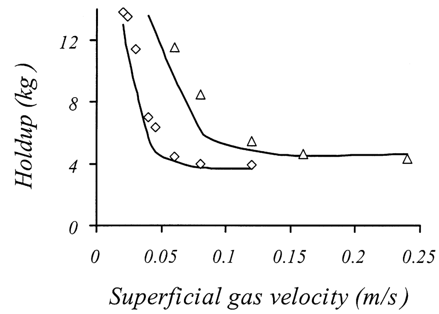

Fig. 14. Influence of the pyrolysis reactor gas velocity on the solids holdup in the pyrolysis reactor for two sand particle diameters ((◇) 220 μm, (△) 390 μm). Operating conditions are listed in Table 3.

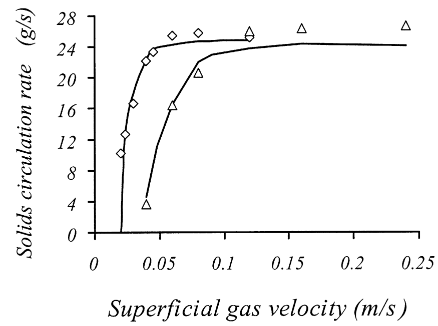

Fig. 15. Influence of the pyrolysis reactor gas velocity on the solids circulation rate for two sand particle diameters ((◇) 220 μm, (△) 390 μm). Operating conditions are listed in Table 3.

ysis reactor and the orifice size on the holdup distribution, orifice gas flow, orifice pressure difference and solids circulation rate. Model and experiment are in fair agreement and the following observations can be made on the influence of the different parameters:

- The orifice size has only a limited influence on the solids circulation rate (Fig. 10). Apparently, a smaller size is largely compensated by a larger holdup in the pyrolysis reactor (Fig. 11) giving a higher pressure difference (Fig. 12). Due to the higher pressure difference, the orifice gas flow increases (Fig. 13).
- The pyrolysis reactor gas velocity only influences the four characteristics mentioned above for $U < U_{mf}$. In this region, an increase in gas velocity results in much higher pressures at the orifice height (Fig. 12) and therefore reduces the necessary solids 'head' above the orifice, giving a lower holdup (Fig. 11). Furthermore, in this region so much sand is transported from the combustor to the pyrolysis reactor that the pressure difference over the standpipe has markedly decreased. When the gas velocity is increased, the pressure difference over the orifice increases resulting in a higher orifice solids flow (Fig. 10). This increases the combustor holdup and the pressure difference over the standpipe thereby installing a higher solids circulation rate.
- Fig. 12 reveals slightly negative pressure differences for the 4 cm orifice. This may be explained by the fact that the pressure was always measured at the height of the orifice centre. For a large orifice, it is possible that because of the bed geometry (i.e., the very narrow bed zone around the rotating shaft), the solids flow preferably through the upper part of the orifice, where a positive pressure difference between the two compartments can still exist.

The combustor gas velocity can not be used to control the solids circulation rate. It was noticed that the solids exchange stopped when the combustor gas flow dropped below U_{mf}. In that case, the pressure forces for solids flow through an orifice are not sufficient to overcome the resistance forces, originating from the solids head above the orifice. In contrary, the solids circulation rate could be controlled by the riser gas velocity and gas flow to the pyrolysis reactor.

Table 4
Fitted discharge coefficients for various orifice diameters

Orifice diameter (cm)	Discharge coefficient
1	0.33
2	0.46
3	0.56
4	0.65

Figs. 14 and 15 show the effect of the pyrolysis reactor gas velocity on the holdup in the pyrolysis reactor and the solids circulation rate for particle diameters of 390 and 220 μm. Clearly, particle size is important. Interesting, when the gas flow in these two figures is normalised to U_{mf}, no influence of the particle diameter is observed. This is an important result if the *IFB*-system under study is applied, e.g., for biomass pyrolysis. In that case, a reduction in particle size is beneficial because of the reduced amount of required fluidizing gas, thereby reducing the dilution of the product gas and the required heat input. Later studies also showed that mixing of the fine biomass particles with the sand was much better for the fine sand, which gives another reason to reduce the sand particle size.

The model could not describe experiments by a single value for the discharge coefficient and had to be fitted for each orifice size (see Table 4). This imperfection may be explained by the complicated flow lines in the small annular space of the pyrolysis reactor between shaft and orifice.

5. Conclusion

A novel solids circulation system is developed which enables the direct coupling of two reactor compartments operating in different gas atmospheres (e.g., reducing and oxidizing). The system consists of an inner compartment in which a fluidised or packed bed is maintained. Solids flow to a surrounding outer compartment through an orifice located close to the gas distributor, as a result of a gas phase pressure difference over the orifice. Solids are recycled from the outer compartment to the inner compartment through a short standpipe, riser and cyclone. This special standpipe/riser-design, with the standpipe submersed in a fluidised bed, results in adequate controllability of the solids flow in the entire system as was shown in experiments in a set-up operating at room temperature and atmospheric pressure. The solids circulation rate is remarkably high (100 kg/h) given the small scale of the set-up.

A model for the *IFB*-system is developed to describe the experimental data. The model combines sub-models for the flow of solids and gas through the orifice and for the flow of solids through the standpipe, in combination with correlated results for the riser hydrodynamics and cyclone pressure difference. The sub-model for flow through an orifice is based on the work of Korbee et al. [4] but the solid phase pressure is discarded as a driving force for solids flow through the orifice.

6. Symbols

a	constant, Eq. (6)
A	area (m^2)
b	constant, Eq. (6)
C	concentration (kg/m^3)
C_d	discharge coefficient
d, D	diameter (m)
E_f	friction losses (Pa)
f	friction factor
g	gravity acceleration (m/s^2)
h_0	height of the virtual tip of the cone, Eq. (7) (m)
h_1	bed height for which $U=U_{mf}$, Eq. (7) (m)
h_s	height of the transition point: conical–cylindrical part, Eq. (7) (m)
h	height (m)
M	holdup (kg)
P	pressure (Pa)
U	superficial gas velocity (m/s)
v	(particle) velocity (m/s)
V	volume (m^3)

Greek symbols

ε	porosity
ε_0	packed bed porosity
η	dynamic viscosity (Pa s)
θ	half cone top angle (°)
ϕ	flow (m^3/s) or (kg/s)
Φ''	flux ($kg/m^2/s$)
ρ	density (kg/m^3)
σ	solids pressure (Pa)
ψ	sphericity factor

Sub- and superscripts

bot	bottom
comb	combustor
cy	cyclone
g	gas or air
in	in (coming)
mf	minimum fluidisation
o, or	orifice
out	out (going)
p	particle
pyr	pyrolysis reactor
s	solid phase
stp	standpipe
sys	total system
x	horizontal direction

Acknowledgements

This investigation was supported by the European Community (CEC-AIR CT93-0889). We thank E.J. Ransdorp, J. Nijmeijer, G. Schorfaar and O.D. Veehof for their assistance in the theoretical and experimental work.

Appendix A

Pressure drop over riser ΔP_r for 390 μm sand

- For a riser gas velocity $u_r < 3.9$ (m/s), $\Delta P_r = -20.66\phi_s + 1055$ (Pa) with ϕ_s the solids flow in (g/s)
- For $3.9 < u_r < 12$ (m/s), $\Delta P_r = (-0.0029u_r^3 + 0.0852u_r^2 - 0.862u_r + 3.42)\phi_s^2 + (-0.12u_r^3 + 3.32u_r^2 - 29.6u_r + 69.4)\phi_s + 1.17u_r^3 - 33.2u_r^2 + 309u_r - 676$

Pressure drop over cyclone ΔP_c for 390 μm sand

$$\Delta P_c = \left(-0.0497 + 0.700\left(1 + (0.111u_r)^{-21.1}\right)^{-1}\right)\phi_s^2 + \left(-24.3 + 31.0\left(1 + (0.106u_r)^{31.5}\right)^{-1}\right)\phi_s + 29.8 + 390\left(1 + (0.104u_r)^{-21.1}\right)^{-1}$$

Pressure drop over riser and cyclone $\Delta P = \Delta P_r + \Delta P_c$ for 220 μm sand

- For $v_r > 3.5$ m/s and $\phi_s > 15$ g/s

$$\Delta P = \phi_s(-0.3538v_r^3 + 9.848v_r^2 - 89.43v_r + 298.3) - 12.517v_r^2 + 237.64v_r - 1523.8$$

- For $\phi_s < 15$ m/s, $\Delta P = 0$.

With the above expressions, the pressure drop over riser and cyclone is described within 10% error.

References

[1] D.S. Scott, J. Piskorz, M.A. Bergougnou, R. Graham, R.P. Overend, The role of temperature in the fast pyrolysis of cellulose and wood, Ind. Eng. Chem. Res. 27 (1988) 8–15.

[2] A. Cuevas, C. Reinoso, D. Scott, The production and handling of WFPP bio-oil and its implications for combustion, in: Proceedings of the biomass pyrolysis oil, properties and combustion meeting, Estes Park, Colorado, USA, 1994, pp. 151–156.

[3] R.G. Graham, B.A. Freel, M.A. Bergougnou, The production of pyrolytic liquids, gas and char from wood and cellulose by fast pyrolysis, in: A.V. Bridgwater, J.L. Kuester (Eds.), Proceedings of Research in Thermochemical Biomass Conversion, Elsevier, New York, 1988, pp. 629–641.

[4] R. Korbee, O.C. Snip, J.C. Schouten, C.M. Van der Bleek, Rate of solids and gas transfer via an orifice between partially and completely fluidized beds, Chem. Eng. Sci. 49 (1994) 5819–5832.

[5] B.M. Wagenaar, W. Prins, W.P.M. Van Swaaij, Pyrolysis of biomass in the rotating cone reactor: modelling and experimental justification, Chem. Eng. Sci. 49 (1994) 5109–5126.

[6] A.M.C. Janse, W. Prins, W.P.M. Van Swaaij, Development of an integrated pilot plant for the flash pyrolysis of biomass, in: A.V. Bridgwater, D.G.B. Boocock (Eds.), Developments in Thermochemical Biomass Conversion, Blackie Academic and Professional, London, 1997, pp. 368–377.

[7] R.H. Venderbosch, A.M.C. Janse, M. Radovanovic, W. Prins, W.P.M. Van Swaaij, Pyrolysis of pine wood in a small integrated pilot plant rotating cone reactor, in: M. Kaltschmitt, A.V. Bridgwater (Eds.), Gasification and Pyrolysis of Biomass: State of the Art and future Prospects, CPL Scientific Ltd., Newbury, UK, 1997, pp. 345–353.

[8] B.M. Wagenaar, W. Prins, W.P.M. Van Swaaij, A.M.C. Janse, Method and apparatus for thermal treatment of non-gaseous material, European Patent PCT/ML96/00327, 1997.

[9] A.M.C. Janse, A heat integrated rotating cone reactor system for flash pyrolysis of biomass, Thesis, University of Twente, Netherlands, 1998.

[10] J.P. Diebold, P. Czernik, F. Scahill, Hot gas filtration to remove char from the pyrolysis vapors produced in the vortex reactor at NREL, in: Proceedings biomass pyrolysis oil, properties and combustion meeting, Estes Park, Colorado, USA, 1994, pp. 90–109.

[11] M. Kuramoto, T. Furasawa, D. Kunii, Development of a new system for circulating fluidized particles within a single vessel, Powder Techn. 44 (1985) 77–84.

[12] M. Kuramoto, D. Kunii, T. Furasawa, Flow of dense fluidized particles through an opening in a circulation system, Powder Techn. 47 (1986) 141–149.

[13] A.H. Masson, A twin fluid bed pyrolyser combustor system, in: J.R Grace, L.W. Shemilt, M.A. Bergougnou (Eds.), Fluidization VI: Proceedings of the international conference on fluidization, Engineering Foundation, New York, 1989, pp. 383–392.

[14] R. Korbee, Regenerative desulfuratization in an interconnected fluidized bed system, Thesis, Delft University of Technology, Netherlands, 1995.

[15] O.C. Snip, The interconnected fluidized bed reactor for gas/solids regenerative processes, Thesis, Delft University of Technology, Netherlands, 1997.

[16] R.W.J. Westerhout, J. Waanders, J.A.M. Kuipers, W.P.M. Van Swaaij, Recycling of polyethene and polypropene in a novel bench-scale rotating cone reactor by high-temperature pyrolysis, Ind. Eng. Chem. Res. 37 (1998) 2293–2300.

[17] R.W.J. Westerhout, J. Waanders, J.A.M. Kuipers, W.P.M. Van Swaaij, Development of a continuous rotating cone reactor pilot plant for the pyrolysis of polyethene and polypropene, Ind. Eng. Chem. Res. 37 (1998) 2316–2322.

[18] L. Massimilla, Flow properties of the fluidized dense phase, in: Fluidization, University of Cambridge, Academic Press, London, 1971.

[19] W.A. Beverloo, H.A. Leniger, J. Van de Velde, The flow of granular solids through orifices, Chem. Eng. Sci. 15 (1961) 260–269.

[20] D.R.M. Jones, J.F. Davidson, The flow of particles from a fluidised bed through an orifice, Rheol. Acta 4 (1965) 180–192.

[21] T.Y. Chen, W.P. Walawender, L.T. Fan, Moving bed solids flow between two fluidized beds, Powder techn. 22 (1979) 89–96.

[22] E.J. Chin, R.J. Munz, J.R. Grace, Dense phase powder feeding from an annular fluidized bed, Powder techn. 25 (1980) 191–202.

[23] M.R. Judd, P.D. Dixon, The flow of fine, dense solids down a vertical standpipe, AIChE Symp. Series 74 (1978) 38–44.

[24] D. Fox, Y. Molodtsof, J.F. Large, Control mechanisms of fluidized solids circulation between adjacent vessels, AIChE J. 35 (1989) 1933–1941.

[25] C.R. Woodcock, J.S. Mason, Bulk Solids Handling, Chapman and Hall, New York, 1987.

[26] J.A.H. De Jong, Vertical air-controlled particle flow from a bunker through circular orifices, Powder Techn. 3 (1969) 267–278.

[27] J.A.H. De Jong, Q.E.J.J.M. Hoelen, Cocurrent gas and particle flow during pneumatic discharge from a bunker through an orifice, Powder Techn. 12 (1975) 201–208.

[28] G.G. Kuvshinov, Free flow of a granular material from an aperture in the presence of a gas counterflow, J. Appl. Mech. Techn. Phys. 36 (1995) 869–876.

[29] J. Molodtsof, A. Ould-Dris, A. Bognar, Particle flow through orifices and solids discharge rates from hoppers, in: O.E. Potter, D.J. Nicklin (Eds.), Fluidization VII: proceedings of the seventh Engineering foundation conference on fluidization, Engineering Foundation, New York, 1992, pp. 361–370.

[30] P.D. Martin, J.F. Davidson, Flow of a powder through an orifice from a fluidised bed, Chem. Eng. Res. Dev. 61 (1983) 162–166.

[31] R.J. Burkett, P. Chalmers-Dixon, P.J. Morris, D.L. Pyle, On the flow of fluidised solids through orifices, Chem. Eng. Sci. 26 (1971) 405–417.

[32] M. Sarkar, S.K. Gupta, M.K. Sarkar, An experimental investigation of the flow of solids from a fluidized bed through an inclined pipe, Powder Techn. 64 (1991) 221–231.

[33] M. Sarkar, S.K. Gupta, M.K. Sarkar, Experimental investigation of solids flow from aerated beds through an inclined pipe, Trans. I. Chem. Eng. 69 (1991) 361–368.

[34] M. Sarkar, S.K. Gupta, M.K. Sarkar, Experimental investigation on gravity flow of solids through inclined standpipes, Chem. Eng. Sci. 46 (1991) 1137–1144.